Macromolecules

Open Access
This article is licensed under CC-BY 4.0

pubs.acs.org/Macromolecules
Article

Hydrophilic Poly(meth)acrylates by Controlled Radical Branching Polymerization: Hyperbranching and Fragmentation

Kriti Kapil, Arman Moini Jazani, Julian Sobieski, Leticia P. Madureira, Grzegorz Szczepaniak, Michael R. Martinez, Adam Gorczyński, Hironobu Murata, Tomasz Kowalewski, and Krzysztof Matyjaszewski*

Cite This: Macromolecules 2024, 57, 5368−5379

Read Online

ACCESS | Metrics & More | Article Recommendations | Supporting Information

ABSTRACT: Topology significantly impacts polymer properties and applications. Hyperbranched polymers (HBPs) synthesized via atom transfer radical polymerization (ATRP) using inimers typically exhibit broad molecular weight distributions and limited control over branching. Alternatively, copolymerization of inibramers (IB), such as α-chloro/bromo acrylates with vinyl monomers, yields HBPs with precise and uniform branching. Herein, we described the synthesis of hydrophilic HB polyacrylates in water by copolymerizing a water-soluble IB, oligo(ethylene oxide) methyl ether 2-bromoacrylate (OEOBA), with various hydrophilic acrylate comonomers. Visible-light-mediated controlled radical branching polymerization (CRBP) with dual catalysis using eosin Y (EY) and copper complexes resulted in HBPs with various molecular weights (M_n = 38 000 to 170 000) and degrees of branching (2%−24%). Furthermore, the optimized conditions enabled the successful application of the OEOBA to synthesize linear-hyperbranched block copolymers and hyperbranched polymer protein hybrids (HB-PPH), demonstrating its potential to advance the synthesis of complex macromolecular architecture under environmentally benign conditions. Copolymerization of hydrophilic methacrylate monomer, oligo(ethylene oxide) methyl ether methacrylate ($OEOMA_{500}$), and inibramer OEOBA was accompanied by fragmentation via β-carbon C−C bond scission and subsequent growth of polymer chains from the fragments. Furthermore, computational studies investigating the fragmentation depending on the IB and comonomer structure supported the experimental observations. This work expands the toolkit of water-soluble inibramers for CRBP and highlights the critical influence of the inibramer structure on reaction outcomes.

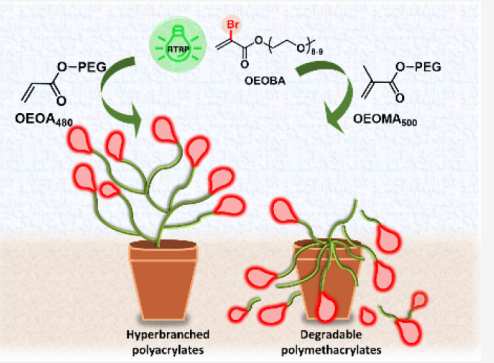

Downloaded via 24.3.243.61 on March 15, 2025 at 04:59:27 (UTC).
See https://pubs.acs.org/sharingguidelines for options on how to legitimately share published articles.

INTRODUCTION

Reversible deactivation radical polymerization (RDRP), also known as controlled radical polymerization (CRP), has received significant attention over the past few decades as it enables the precise synthesis of macromolecules with predetermined molecular weight, narrow molecular weight distribution, controlled topology, composition, and functionality.[1−9] Notably, polymer topology is a crucial attribute that impacts the solution/melt viscosity, glass transition temperature, solubility in diverse solvents, and size of individual polymer chains in solution.[10−16] RDRP facilitates the development of advanced functional materials with well-defined architecture, including densely grafted linear copolymers,[17] star copolymers,[18] bottlebrush copolymers,[19,20] hyperbranched polymers,[21−23] networks/gels,[24,25] and cyclic copolymers,[26] suitable for an extensive range of applications such as nanocomposites,[27] and biomedical uses, including drug delivery systems[28,29] and scaffolds.[30−32]

Structurally controlled hyperbranched polymers (HBPs) exhibit distinctive physical properties, such as weaker entanglements, lower intrinsic viscosity, multiple modifiable end-groups, and the presence of cavities.[33,34] Consequently, HBPs emerge as the most promising alternatives to dendrimers, circumventing the tedious multistep synthesis.[35,36] However, achieving structural control in the synthesis of HBPs remains a practical challenge. Methods like step-growth polymerization through polycondensation of AB_x monomers or A_2+B_x monomers,[37−41] or by self-condensing vinyl polymerization (SCVP) using AB* inimer containing a double bond (A) and initiating group (B*) result in HBPs with limited control over molecular weight, dispersity, and degree of branching.[11,21−23,42−44] While specific conditions such as gradual addition of more reactive monomer,[45] *in situ* modulations of monomer reactivity through substitution,[37] microemulsion polymerization,[46,47] or click polymeriza-

Received: February 19, 2024
Revised: May 8, 2024
Accepted: May 16, 2024
Published: May 29, 2024

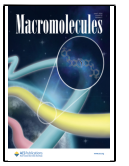

© 2024 The Authors. Published by American Chemical Society

Scheme 1. (A) IB Used for CRBP Developed in Previous Work and this Work. (B) Proposed Pathway for Aqueous CRBP to Synthesize HB Polyacrylates Using EY-ATRP. (C) Components of the ATRP Reaction Mixture

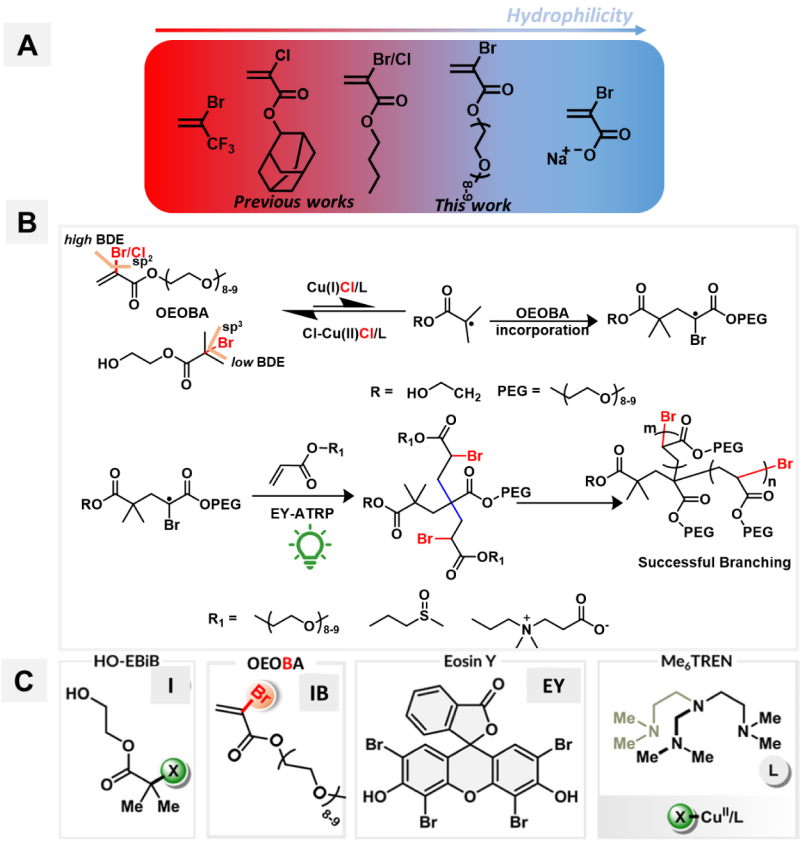

tion,[48−50] have proven effective in achieving control, but they substantially restrict the range of monomers and polymerization conditions available.[51]

Yamago and Zhong have recently introduced a novel and generalized approach for advancing organotellurium-mediated radical polymerization (TERP)[52] and atom transfer radical polymerization (ATRP)[53] toward the synthesis of hyperbranched polymers (HBPs). In the conventional AB* inimer system, which exhibits distinct reactivity for A and B* functional groups, it often results in the formation of highly dispersed HBPs. To enhance structural control, novel branching monomers with hierarchical reactivity were engineered. These monomers, coined as "inibramers (IB)" by Zhong, and "evolmers" by Yamago can trigger the branching process only after their incorporation into the polymer chain. The inibramer/evolmer contains a vinyl halide/telluride bond (C(sp^2)−X, where X = Cl or Br or TeR) at the α position. This bond has a notably high bond dissociation energy (BDE), rendering it unreactive under typical ATRP or TERP conditions. Nevertheless, once the inibramer is incorporated into the propagating chain, the resulting C(sp^3)−X bond with a lower BDE can be activated, instigating the initiation of a new branch (Scheme 1B). Zhong demonstrated unprecedented control over the branching of acrylates, styrene, acrylonitrile, and acrylamides, using hydrophobic inibramer such as α-bromo/chloro butyl acrylate in organic solvents.[54] Chen et al. also reported a one-pot synthesis of well-defined branched fluoropolymers using 2-bromo-trifluoropropene IB (Scheme 1A).[55] However, both of these methods suffer from the high inibramer reactivity ratio and challenges in regulating copolymerization kinetics.

Our group extended the application of ATRP method in water using a water-soluble ionic inibramer sodium 2-bromoacrylate (SBA) with improved copolymerization kinetic parameters to synthesize hydrophilic hyperbranched polymethacrylates.[56] TERP under emulsion conditions in water using Brij 98 surfactant for the synthesis of highly branched poly(*n*-butyl acrylate) was reported.[57]

ATRP of acrylates in water is still considered a challenge due to potential hydrolysis of the C(sp^3)−X (secondary halides are more prone to hydrolysis than tertiary), leading to loss of chain-end functionality since the C(sp^3)−OH cannot participate in further chain growth.[58−60] Second, the high values of equilibrium constant of ATRP in water lead to a high concentration of radicals, which may result in more dead chains.[61,62] These challenges shall be even more pronounced during the controlled synthesis of hyperbranched acrylates using inibramers because their incorporation enhances the concentration of radicals.[63,64] Recently, we extended the scope EY/Cu photocatalyzed ATRP[65] resulting in well-defined water-soluble linear acrylates under biorelevant conditions[66−68] using low-energy green light.[69,70] The use of Cu^{II}/Me_6TREN as deactivator and EY at ppm levels in 1× phosphate-buffered saline (PBS) medium suppressed the dissociation of the $[X−Cu^{II}/L]^+$ deactivators and disproportionation of Cu^I species to Cu^{II} and Cu^0 thereby maintaining equilibrium throughout ATRP.

In this study, we aimed to expand the library of water-soluble IBs to advance CRBP in water. A water-soluble PEG-

https://doi.org/10.1021/acs.macromol.4c00408
Macromolecules 2024, 57, 5368−5379

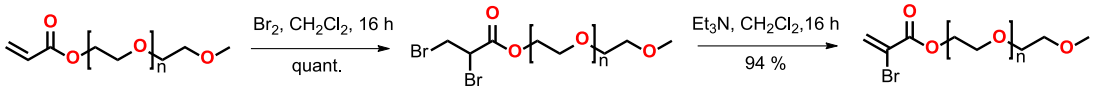

Figure 1. Synthesis of IB oligo(ethylene oxide) methyl ether 2-bromoacrylate (OEOBA).

Table 1. Synthesis of HB-Polyacrylates by Copolymerization of OEOBA and Hydrophilic Acrylate Monomers: $OEOA_{480}$, CBA, MSEA[a]

entry	[M]/[OEOBA]/[I]	feed rate (eq/min)	α_M[b] (%)	α_{IB}[b] (%)	$M_{n,th}$[c] ([I])	$M_{n,abs}$[d]	$Đ$
1	200/12/1	batch	55	>99	55 000	54 500	1.16
2	200/0/1	-	82	-	78 720	84 000	1.09
3	200/4/1	0.06	86	>99	84 800	84 600	1.60
4	200/8/1	0.133	90	>99	90 900	94 200	1.58
5	200/12/1	0.2	85	>99	88 300	92 200	1.55
6	200/24/1	0.3	82	>99	88 800	84 400	1.48
7[e]	200/24/1	0.2	92%	>99	56 900	53 700	1.83
8[f]	200/12/1	0.2	97%	>99	47 000	50 300	1.40
9	100/6/1	0.2	67%	>99	35 500	38 300	1.56
10	400/24/1	0.2	60%	>99	128 600	123 000	1.48
11	600/36/1	0.2	52%	>99	170 100	169 000	1.52

[a]Reaction conditions: [M]/[OEOBA]/[HO-EBIB]/[EY]/[$CuBr_2$]/[Me_6Tren]: 200/0-24/1/0.01/0.2/0.3, M = OEOA480, MSEA[d] CBA[e] [OEOBA] = 0−36 mM, [HO-EBIB] = 0.5−1.5 mM in 1× PBS buffer at room temperature, irradiated with green light LEDs (λ_{max} = 527 nm, 50 mW cm^{-2}), without deoxygenation for 60 min. Reaction volume 2.0 mL, stirring at 100 rpm. [b]a$OEOA_{480}$ and OEOBA conversion was determined by using ^{1}H-NMR spectroscopy. [c]Theoretical molecular weight was calculated using the equation $M_{n,th}$ = [M/I] * MW_M *αM + [OEOBA/I]* MW_{OEOBA}* αIB +MW_I. [d]$M_{n,abs}$ and $Đ$ were analyzed using SEC (1× PBS as eluent) equipped with triple detectors: multi-angle light scattering (MALS), refractive index (RI), and inline viscometer and UV detector. [e]MSEA was used as a monomer. [f]CBA was used as a monomer.

based IB, namely, oligo(ethylene oxide) methyl ether 2-bromoacrylate acrylate (OEOBA) was synthesized. This approach facilitated rapid and well-controlled aqueous branching polymerizations of hydrophilic acrylates under homogeneous conditions in open air under green light. While careful optimization resulted in the successful synthesis of hydrophilic HB polyacrylates, the PEG side chain of the IB was less efficient for the synthesis of HB polymethacrylates. This was attributed to the accelerated fragmentation of the polymethacrylate backbone by midchain radicals (MCR).

RESULTS AND DISCUSSION

Synthesis of PEG-Based IB. The new water-soluble PEG-based IB was synthesized in two steps using oligo(ethylene oxide) methyl ether acrylate (M_n = 480) as the starting material in a one-pot reaction (Figure 1). The addition of bromine (Br_2) to the double bond resulted in the formation of 2,3-dibromo oligo(ethylene oxide) methyl ether acrylate in quantitative yield. Following the removal of excess Br_2, this intermediate was directly employed in a subsequent step. Triethylamine allowed for a mild elimination reaction, with selective removal of the β-bromine, to form the final product, oligo(ethylene oxide) acrylate methyl ether 2-bromoacrylate (OEOBA) (see Supporting Information). Progress of the reaction was monitored by ^{1}H NMR spectroscopy, while the structures of intermediates and final monomer were conclusively confirmed by ^{1}H and ^{13}C NMR spectra (Figures S1−S5). The final compound was moderately stable and was stored at 4 °C, which is a common characteristic among IB-type monomers.[53]

Synthesis of HB Polyacrylates. To synthesize HB-$POEOA_{480}$, we performed copolymerization of oligo(ethylene oxide) methyl ether acrylate (average M_n = 480, $OEOA_{480}$) with OEOBA using oxygen-tolerant EY/Cu^{II}-tris[2-(dimethylamino)ethyl]amine (Me_6TREN) dual-catalyzed photo redox ATRP. The copolymerization was carried out in the presence of 2-hydroxyethyl α-bromoisobutyrate (HO-EBIB) as the initiator (Table 1) in phosphate-buffered saline (PBS) as the reaction medium to provide biocompatible conditions to suppress dissociation of the $[X-Cu^{II}/L]^+$ deactivator and to form the highly photoactive form of EY (Scheme 1C). The polymerizations were carried out in open vials placed in a photoreactor with green LEDs (527 nm, 50 mW cm^{-2}). The copolymerization of $OEOA_{480}$ (300 mM) and OEOBA (18 mM), conducted in the batch process, resulted in a high conversion of OEOBA inibramer (>99%), but a relatively lower conversion of comonomer, $OEOA_{480}$ (55%) in 60 min (Table 1, entry 1). This indicated that gradient copolymers were synthesized in a batch process due to IB's higher reactivity than the $OEOA_{480}$ (Figure S6). Similar observations were reported earlier for ATRP in organic media.[54]

To enable statistical incorporation of OEOBA and thus achieve randomly distributed branching junctions along the polymer backbone, OEOBA was introduced to the polymerization by feeding over 60 min in the subsequent reactions. The molar ratio of OEOBA varied from 2 to 12 mol % to achieve a tunable degree of branching in the synthesized HB-polyacrylates (Table 1, entries 3−6). ^{1}H NMR revealed high conversion of both $OEOA_{480}$ and OEOBA. Analysis of the resulting copolymer by size-exclusion chromatography (SEC) with a multiangle light scattering (MALS) detector revealed that the absolute molecular weight ($M_{n,abs}$) of copolymers agreed well with their theoretical molecular weights ($M_{n,th}$). Furthermore, the HB-$POEOA_{480}$ also possessed slightly higher dispersity values than their linear counterpart (Table 1, entry 2), arising from the broader branching distribution along the polymer backbone (Figure S7).[54,71] The copolymerization kinetics of OEOBA with $OEOA_{480}$ under these conditions revealed that the $M_{n,abs}$ of HB polyacrylates increased as a function of monomer conversion (Figure S8A−C), and agreed well with $M_{n,th}$. The molecular weight distribution values also

https://doi.org/10.1021/acs.macromol.4c00408
Macromolecules 2024, 57, 5368−5379

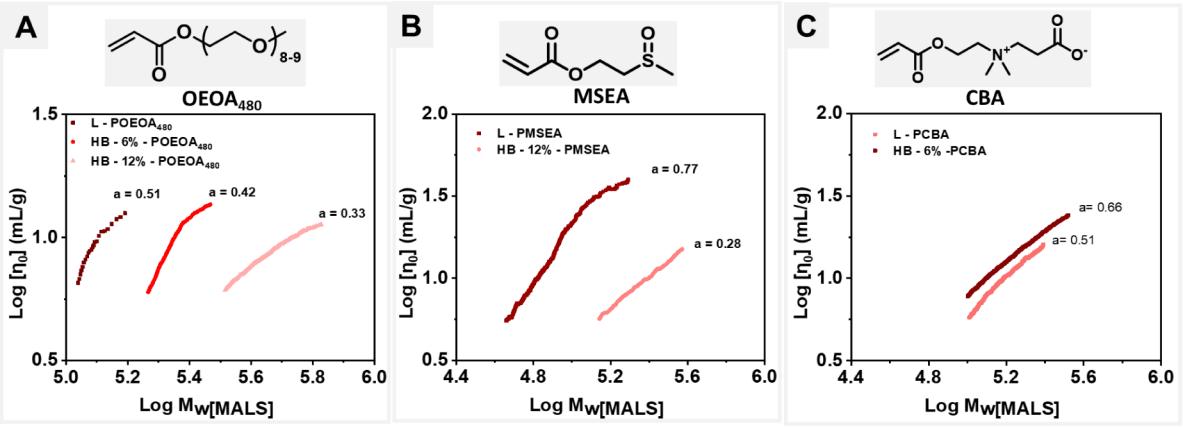

Figure 2. Intrinsic viscosity as a function of molar mass where L refers to linear analogs of (A) HB-POEOA$_{480}$, (B) HB-PMSEA, and (C) HB-PCBA. The slope values, known as Mark–Houwink parameter "a", correspond to the polymer conformation.

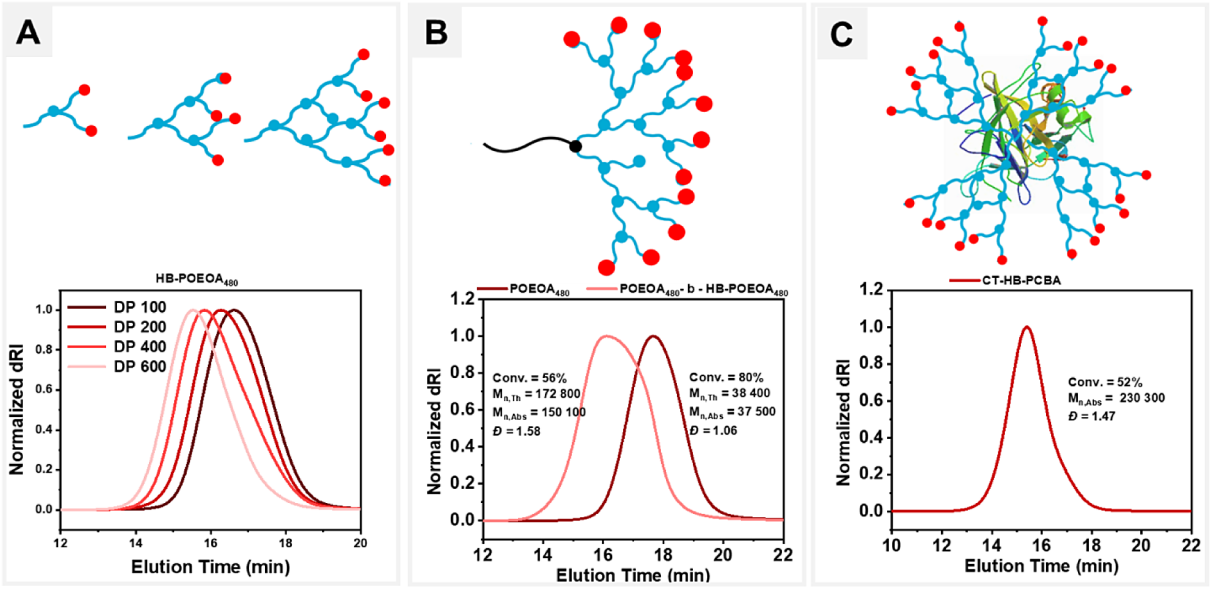

Figure 3. Synthetic scope of HB polyacrylates; (A) varying targeted degree of polymerization (DP), (B) *in situ* chain extension to form linear-HB block copolymer. (C) Synthesis of HB-PPH using CT to form CT-HB-PCBA.

increased as a function of the degree of branching ($1.22 \leq Đ \leq 1.69$) during polymerization (Figure S8C).

Expanding Monomer Scope. The scope of monomers was further expanded to include other water-soluble acrylates. Copolymerization of the OEOBA with 2-(methyl sulfinyl) ethyl acrylate (MSEA) and zwitterionic carboxy betaine acrylate (CBA) afforded well-defined branched polymers with predicted molecular weights (Table 1, entries 7 and 8) and broad molecular weight distributions, that could be attributed to hyperbranched structures (Figure S9).[71] Furthermore, hydrophobic monomers such as methyl acrylate (MA) and ethyl acrylate (EA) were also copolymerized with the OEOBA inibramer (see Supporting Information). Due to the amphiphilic properties of OEOBA, HB-PMA and HB-PEA were synthesized with good control in DMSO within 90 min under green LEDs (527 nm, 50 mW cm^{-2}) without prior deoxygenation (Figure S10). This demonstrated that the catalytic system described herein can also be extended to the nonaqueous polymerization system for hydrophobic monomers.

To characterize the degree of branching, the molar mass and the molecular size were determined simultaneously and independently using SEC-MALS equipped with a triple detector (UV, RI, Viscometer) and inline DLS. A Mark–Houwink–Sakurada (MHS) plot showing intrinsic viscosity as a function of molar mass (log–log plot of $[\eta]$ versus M), revealing the polymer conformation, was obtained (Figure 2A). The slope of HB-POEOA$_{480}$ had lower values as compared to linear POEOA$_{480}$ as indicated by the MH constant "a". Also, subsequent reduction in "a" values was observed for a higher molar ratio of inibramer, confirming the successful synthesis of well-defined hyperbranched polyacrylates with tunable branching ratio.[35,72] Similar MHS plots for HB-PMSEA (Figure 2B) and HB-PCBA (Figure 2C) also revealed a lowering in slope values ("a") as a function of the degree of branching.

Varying Targeted Degrees of Polymerization (DP). The degree of polymerization was varied (DP = 100–600) to obtain HB polymers with variable molecular weights and degrees of branching. The polymerization was carried out by varying the HO-EBIB concentration while keeping the

https://doi.org/10.1021/acs.macromol.4c00408
Macromolecules 2024, 57, 5368–5379

Table 2. Copolymerization of $OEOMA_{500}$ with OEOBA[a]

entry	[M]/[IB]/[I]	α_M[b] (%)	α_{IB}[b] (%)	$M_{n,th}$[c] ([I])	$M_{n,app}$[d]	$M_{n,abs}$[e]	$Đ$
1.	200/4/1	93	>99	87 600	23 400	32 000	1.20
2.	200/12/1	83	>99	80 800	11 000	16 000	1.17
3.	200/0/1	88	-	88 200	60 000	90 000	1.06

[a]Reactions conditions: $[OEOMA_{500}]/[OEOBA]/[HO\text{-}EBIB]/[EY]/[CuBr_2]/[TPMA]$: 200/12/1/0.01/0.2/0.6, $[OEOMA_{500}]$ = 300 mM, [OEOBA]= 6−18 mM, [HOBIB] = 1.5 mM in 1× PBS buffer at room temperature, irradiated for 30 min under green light LEDs (λ_{max} = 520 nm, 9.0 mW cm^{-2}) without deoxygenation. Reaction volume 4.4 mL. [b]a$OEOMA_{500}$ and OEOBA conversions were determined by using ^{1}H NMR spectroscopy. [c]$M_{n,th}$ was calculated using the equation $M_{n,th}$ =[M/I] * $MW_{OEOMA50}$0 *α_M + [OEOBA/I]* MW_{OEOBA}* α_{OEOBA} +$MW_{HO\text{-}EBIB}$. [d]$M_{n,app}$ analyzed using GPC (DMF as an eluent), calibrated with PMMA standards. [e]$M_{n,abs}$ analyzed using SEC (1× PBS as eluent) equipped with triple detectors: MALS, RI and inline viscometer and UV detector.

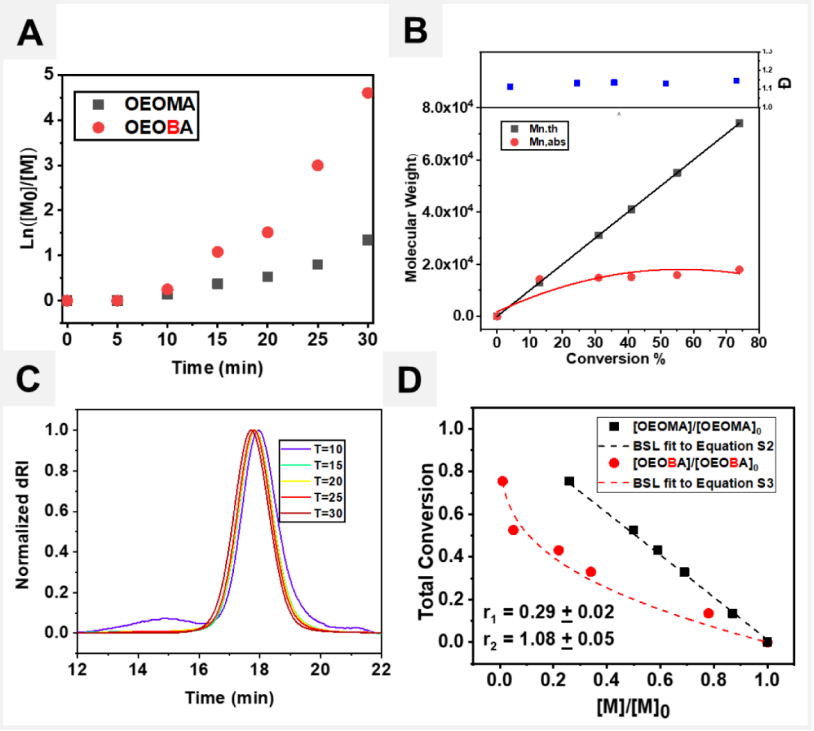

Figure 4. Copolymerization kinetics using molar ratios $[OEOMA_{500}]/[OEOBA]/[HO\text{-}EBIB]/[EY]/[CuBr_2]/[TPMA]$ = 200/12/1/0.01/0.2/0.6. (A) First-order kinetic plot. (B) Evolution of molecular weight and molecular weight distribution with % conversion-depict poor control. (C) SEC traces evolution with time depict no shifts. (D) BSL curve fitting to kinetics experiments depicts 4× higher reactivity ratio.

concentrations of the other reagents constant and slowly feeding the OEOBA for 60 min (Table 1, entries 9−11). HB-$POEOA_{480}$ exhibited predictable $M_{n,abs}$ and broader molecular weight distribution ($Đ \leq 1.56$), typical for a branched polymer (Figure 3A).[71] Lack of deviations from $M_{n,th}$ suggests the absence of new polymer chains or backbone fragmentation, contrary to observations below with polymethacrylate backbones.[56]

Linear-HB Topological Block Copolymer Synthesis. Next, an *in situ* chain extension experiment was performed to analyze the chain-end fidelity. The linear $POEOA_{480}$ macroinitiator (conv. = 80%, $M_{n,abs}$ = 37 500, $Đ$ = 1.06) was synthesized (see Supporting Information). A sample was taken from the postpolymerization mixture and used without further purification to prepare a new reaction mixture containing the $OEOA_{480}$ (300 mM). After 60 min of slowly feeding OEOBA (18 mM) and of green light irradiation (λ_{max} = 527 nm, 50 mW cm^{-2}), in an ambient temperature, $OEOA_{480}$ conversion was 56%. The SEC-MALS analysis showed a clear shift toward higher molecular weights without any shoulder or tailing at lower molecular weights ($M_{n,abs}$ = 150 100, $Đ$ = 1.58), indicating a controlled polymerization and high retention of chain end functionality (Figure 3). The absence of a low molecular weight shoulder in SEC traces indicated negligible fragmentation and successful chain extension from the macroinitiator, resulting in linear-HB topological block copolymer.

Synthesis of HB-Protein Polymer Hybrids (PPH). Owing to the benign condition of EY/Cu catalyzed aqueous CRBP, the grafting-from approach was applied to graft HB-PCBA from the surface of chymotrypsin (CT) enzyme, functionalized with 12 ATRP initiators, to achieve tunable molecular sieving.[73] HB-PCBA was grafted from the CT macroinitiator.[74] The copolymerization of CBA (300 mM) and OEOBA (18 mM) fed at the rate of 0.2 eq/min was carried out in a Lumidox photoreactor (527 nm, 125 mW/cm^2) at 15−18 °C to preserve the activity of CT. The purified bioconjugate was analyzed by ^{1}H NMR (conv. = 52%) and SEC-MALS ($M_{n,abs}$ = 230 300, $Đ$ = 1.47) (Figure 3). High molecular weight and monomodal molecular weight distribution indicated a well-controlled branching polymerization.

https://doi.org/10.1021/acs.macromol.4c00408
Macromolecules 2024, 57, 5368−5379

Scheme 2. Proposed Mechanism for the (A) Copolymerization of $OEOMA_{500}$ and OEOBA. (B) β-Carbon Fragmentation of Radical Intermediates

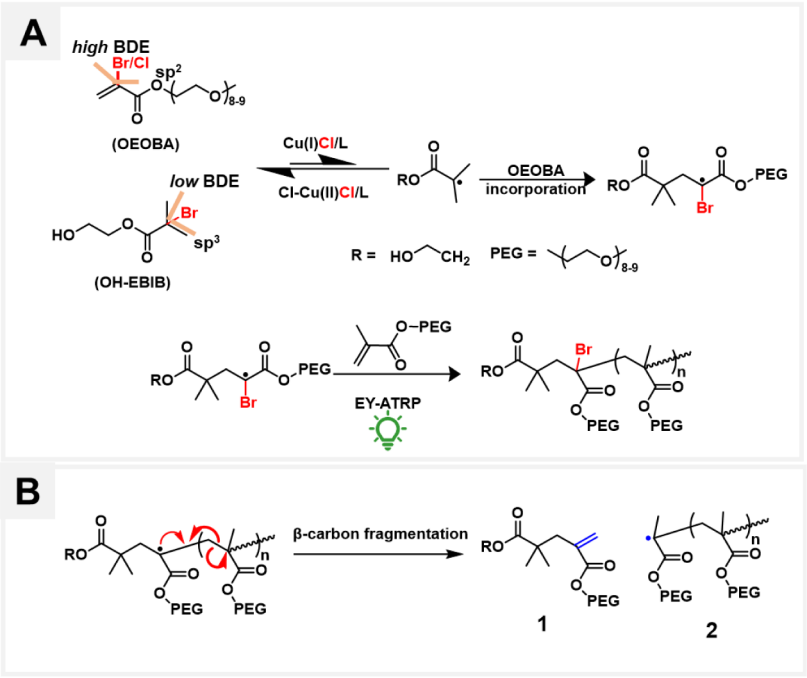

Copolymerization of OEOBA with $OEOMA_{500}$. Encouraged by the successful CRBP of $OEOA_{480}$, we employed an OEOBA to synthesize HB hydrophilic polymethacrylates. The copolymerization of OEOBA and a methacrylate comonomer, oligo(ethylene oxide) methyl ether methacrylate (average M_n = 500, $OEOMA_{500}$), was performed using molar ratios of $[OEOMA_{500}]/[OEOBA]/[HO\text{-}EBIB]/[EY]/[CuBr_2]/[TPMA]$ = 200/4/1/0.01/0.2/0.6. High conversions of $OEOMA_{500}$ and OEOBA were observed within 30 min (Table 2, entry 1). The apparent molecular weight of the resulting copolymer ($M_{n,app}$ = 23 400) determined by SEC calibrated with linear poly(methyl methacrylate) standards was significantly lower than the $M_{n,th}$ value (Figure S11A). The lower $M_{n,app}$ values than $M_{n,th}$ values are typical for HBPs due to the lower hydrodynamic volume. Nevertheless, analysis of the resulting copolymer by SEC with a MALS detector revealed that the $M_{n,abs}$ of the copolymer was also much lower than that of the $M_{n,th}$ (Figure S11B). In addition, the resultant copolymer had a narrow molecular weight distribution ($Đ$ = 1.20) when compared to that of HB-$POEOA_{480}$ of the same OEOBA and $OEOA_{480}$ feed ratio ($Đ$ = 1.60). Copolymerization with a higher molar ratio (6 mol %) of OEOBA (Table 2, entry 2) resulted in an even lower value of measured $M_{n,app}$, and $M_{n,abs}$ values, despite the high conversion of both OEOBA and $OEOMA_{500}$, as determined by ^{1}H NMR. The homopolymerization of $OEOMA_{500}$ resulted in a well-controlled linear polymer consistent with previous observations (Table 2, entry 3).[65] The low molecular weight polymers indicated unsuccessful branching in the case of methacrylate, which was further verified by following the copolymerization kinetics of $OEOMA_{500}$ and OEOBA and the synthesis of model polymers with halogens in the backbone.

The copolymerization kinetics of $OEOMA_{500}$ and OEOBA was monitored by performing the polymerization reaction under same conditions as above (Table 1, entry 2) using molar ratios as follows: $[OEOMA_{500}]/[OEOBA]/[HO\text{-}EBIB]/[EY]/[CuBr_2]/[TPMA]$ = 200/12/1/0.01/0.2/0.6). The samples were drawn out at regular intervals (5 min), quenched with 1,4-bis(3-isocyanopropyl) piperazine,[75] and then analyzed by ^{1}H NMR and SEC-MALS. The copolymerization exhibited first-order kinetics with a short induction period of 5 min, followed by a rapid polymerization, reaching 78% and >99% of $OEOMA_{500}$ and OEOBA conversion within 30 min, respectively (Figure 4A). The rate of the conversion of OEOBA was higher than that of the conversion of $OEOMA_{500}$, suggesting the gradient incorporation of the conversion of OEOBA. The polymer samples showed no increase in the observed $M_{n,abs}$ values with an increase in the monomer conversion (Figure 4B). In addition, SEC revealed overlapping traces and did not show any shift in the elution time with increasing monomer conversion. However, they remained narrow throughout polymerization (Figure 4C). The Beckingham–Sanoja–Lynd (BSL)[76] copolymerization model used to estimate the reactivity ratio, revealed 4 times higher reactivity of OEOBA inibramer as compared to $OEOMA_{500}$ ($R_{1,OEOMA}$ = 0.29, $R_{2,OEOBA}$ = 1.08 Figure 4D). This is in agreement with previously observed higher reactivity ratio of IB relative to butyl acrylate,[53] but unlike comparable reactivity ratio between $OEOMA_{500}$ and SBA.[56]

Analysis of $POEOMA_{500}$ Fragmentation Through Br-Activated MCR. The lower-than-expected molecular weights can be attributed to the β-carbon fragmentation of the $POEOMA_{500}$ backbone via formation of midchain radicals (MCRs) upon activation of C–Br bond (Scheme 2).[77,78] The MCRs generated from C–Br bonds in the backbone of polyacrylates were sufficiently stable to synthesize graft/brush copolymers,[79] whereas the polymethacrylates underwent fragmentation using ruthenium or photocatalysts.[80−82]

To investigate this under our polymerization conditions, two model copolymers of $OEOMA_{500}$ and OEOBA were synthesized using sodium pyruvate (SP)-reversible addition–fragmentation (RAFT) polymerization with different feed

https://doi.org/10.1021/acs.macromol.4c00408
Macromolecules 2024, 57, 5368−5379

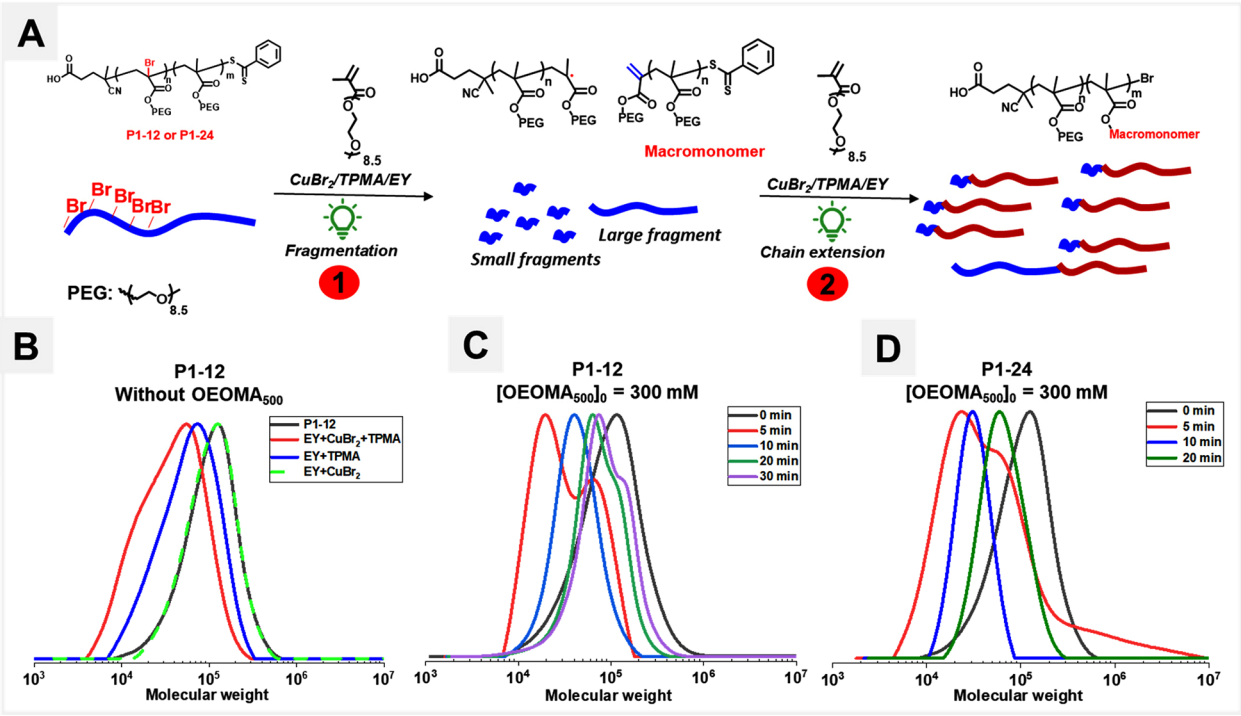

Figure 5. (A) Two steps fragmentation of Br-activated MCR in POEOMA$_{500}$-co-POEOBA copolymers and chain extension from fragmented chains during EY-ATRP. (B) SEC traces of P1−12 in the absence of OEOMA$_{500}$. (C) SEC traces of P1−12 in the presence of OEOMA$_{500}$ (D) SEC traces of P1−24 in the presence of OEOMA$_{500}$.

ratios of OEOBA (target DP of OEOBA = 12 and 24), yielding POEOMA$_{500}$ copolymers (P1−12 and P1−24) with midchain Br atoms (Figure 5). The successful one-pot synthesis of copolymers was confirmed (^{1}H NMR and SEC in Figures S13 and S14) and no activation of C−Br was observed during RAFT polymerization.[83,84] The higher reactivity of OEOBA versus that of OEOMA$_{500}$ affords gradient copolymers with rich C−Br sequences at the beginning of chains.[85]

The copolymers were then exposed to EY-ATRP conditions to generate radicals by activating C−Br (Figure 5A). Upon exposing P1−12 to green light irradiation in the presence of $CuBr_2$, TPMA, and EY (without monomer), the SEC traces shifted to a lower molecular weight region ($M_{n,app}$ before irradiation = 92 000, $Đ$ = 1.42; $M_{n,app}$ after irradiation = 26700, $Đ$ = 1.91), suggesting the homolytic cleavage of C−C bonds through the MCR formation (Figure 5B). Degradation of P1−12 also occurred in the absence of metal ($CuBr_2$), and only in the presence of EY and TPMA ($M_{n,app}$ after irradiation = 49 000, $Đ$ = 1.66). However, the SEC traces remained nearly unchanged in the presence of EY and $CuBr_2$ (without an electron donor, TPMA) or with EY alone, even after prolonged irradiation (16 h) in deoxygenated media (Figure S15). This suggests that EY-catalyzed C−Br activation of midchain halogens primarily occurs through a reductive quenching mechanism involving electron transfer (ET) from TPMA amines to EY, followed by C−Br activation through electron transfer from EY. The degradation of P1−12 did not yield low molecular weight fragments corresponding to 12 times lower molecular weight species. This can be attributed to the higher reactivity ratio of OEOBA versus OEOMA$_{500}$ (as mentioned earlier), resulting in the gradient incorporation of OEOBA during one-pot RAFT copolymerization.

We hypothesized that the presence of monomers (OEOMA$_{500}$) might suppress fragmentation by reacting with radicals formed in the backbone, thereby promoting the generation of brush copolymers over fragmentation (Figure S12). To investigate this, a midchain C−Br activation experiment for P1−12 and P1−24 was conducted in the presence of all polymerization components ($CuBr_2$+TPMA +EY) along with OEOMA$_{500}$ (300 mM), and the process was monitored over time. Under this condition, after 5 min of irradiation, both P1−12 and P1−24 exhibited degradation, as evidenced by the formation of lower molecular weight species in SEC (Figure 5C,D) and ^{1}H NMR (Figure S16), followed by a gradual increase in SEC traces toward the higher molecular weight region, as the polymerization progressed. This unequivocally indicated that fragmented chains acted as initiators to form new chains (Figure 5A), resulting in polymers with a final $M_{n,abs}$ lower than $M_{n,th}$. Notably, β-carbon fragmentation yielded two polymer species: one with a radical and another with an unsaturated end chain (macromonomer), which can either initiate or be incorporated into new polymer chains. Attempts to suppress fragmentation by using higher monomer concentrations ([OEOMA$_{500}$]$_0$ = 800 mM) led to gelation. This revealed that MCR-induced fragmentation is a predominant event in polymethacrylates and cannot be prevented under these experimental conditions.

To suppress the rate of fragmentation, thereby increasing the structural control in HB polymethacrylates synthesized by TERP, low-temperature conditions were reported to be more suitable.[77] To achieve successful branching, EY/Cu-mediated ATRP was then performed under low-temperature conditions with slow feeding of the OEOBA inibramer. The copolymerization kinetics was slower as the polymerizations were carried out at 12 °C and further lower at 5 °C as revealed by the conversion of the monomer measured by ^{1}H NMR (Table S2). However, SEC-MALS analysis of resultant copolymers showed only a very small improvement in the observed $M_{n,abs}$

https://doi.org/10.1021/acs.macromol.4c00408
Macromolecules 2024, 57, 5368−5379

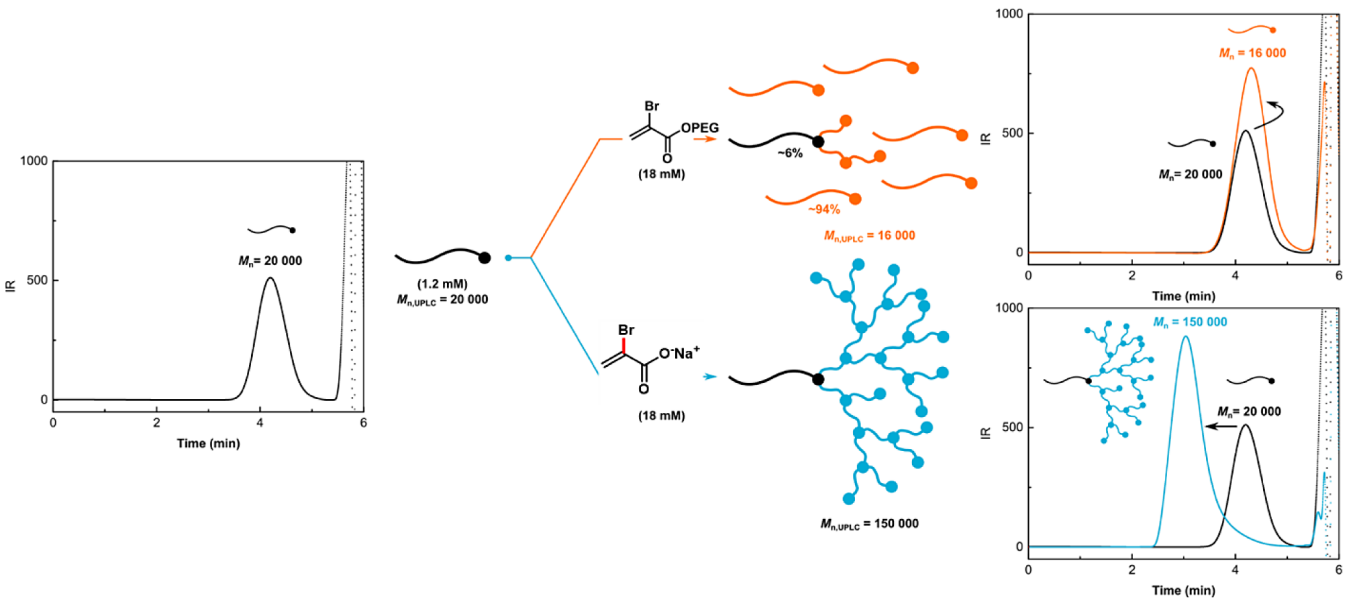

Figure 6. Comparison between OEOBA and SBA in an *in situ* chain extension experiment toward synthesis of POEOMA$_{500}$-*b*-HB-POEOMA$_{500}$.

as compared to copolymerization conducted at 25 °C. There still was poor agreement between $M_{n,th}$ and $M_{n,abs}$. The SEC traces did not shift to higher molecular weight regions with an increase in conversion of the OEOMA$_{500}$ (Figure S17). This indicated that the rate of propagation and, hence, successful branching event competed with the rate of fragmentation because of the instability of the polymer backbone due to the incorporated inibramer.

Comparison between OEOBA and SBA During Copolymerization with OEOMA$_{500}$. To compare the performance of OEOBA and the previously reported SBA inibramer[56] during copolymerization with OEOMA$_{500}$, an *in situ* chain extension experiment was conducted using a linear POEOMA$_{500}$ ($M_{n,abs}$ = 20 000) as a macroinitiator which was further extended with a second block using either OEOBA or SBA with OEOMA$_{500}$. Ultraperformance liquid chromatography (UPLC) analysis of resultant copolymers indicated no shift in the trace of macroinitiator when the OEOBA was used. Conversely, SBA enabled grafting of HB-POEOMA$_{500}$ block as revealed by a clear shift of polymer trace (Figure 6). This highlights the critical role of the IB structure in the CRBP. The SBA, with a short ionic side chain, promotes rapid propagation of radicals instead of fragmentation of the polymethacrylate backbone, whereas the OEOBA, with the relatively longer side chain of PEG, resulted in fragmentation.

Computational Analysis of Total Energies for Model Substrates and Fragments. To gain insight into the fragmentation tendency, computational studies were carried out on model inibramer substrates with surrounding acrylates and methacrylates. Reactants and products were designated within the activation and *β*-scission reactions (Scheme 3a,b). Through the course of the overall reaction sequence, monomer−inibramer−-monomer (i.e., symmetric trimeric species of ABA, where A = comonomer and B = IB) model alkyl halides substrate (MCR-Br) was activated to form MCR and atomic Br, whereby MCR fragmented into radical (RF) and unsaturated (U) fragments. The energy coordinate diagram for the activation-scission pathway for model compounds is shown in Scheme 3c. Total energies were compiled, and the reported relative energies follow the following equations:

Scheme 3. Model Substrates Bearing a Central Inibramer Unit Flanked by either Acrylate- or Methacrylate-based Moieties[a]

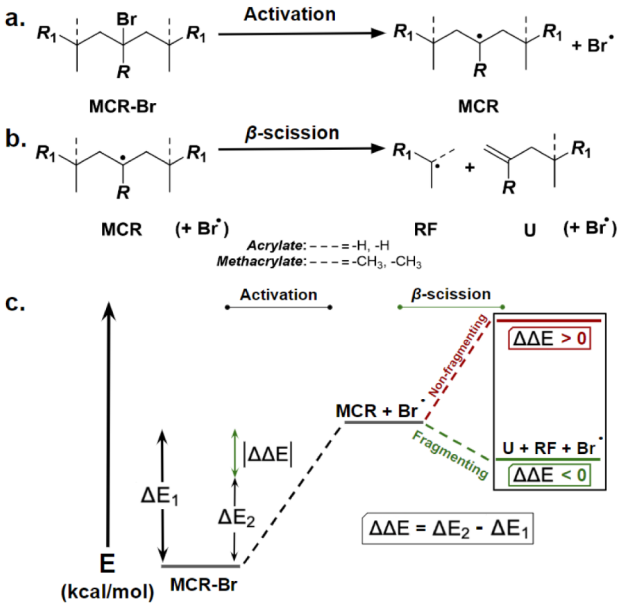

[a]The activation reaction of a model midchain alkyl halide (MCR-Br) to form a Br atom and MCR. (b) The *β*-scission reaction of an MCR forming corresponding radical fragment (RF) and unsaturated (U) species (Br atom is considered stoichiometrically for total energies but is not a reactant). (c) Energy reaction coordinate diagram for the substrates and products of the above reactions, with favorable (green) and unfavorable (red) fragmentation pathways based on calculated $\Delta\Delta E$ values. ΔE_1 is the difference in total energies between activated intermediate product and starting alkyl halide substrate, ΔE_2 is the difference in total energy between *β*-scission products and starting alkyl halide substrate, and $\Delta\Delta E$ is the difference between ΔE_2 and ΔE_1, shown (green arrow) as an absolute value.

https://doi.org/10.1021/acs.macromol.4c00408
Macromolecules 2024, 57, 5368−5379

$$\Delta E_1 = (E_{MCR} + E_{Br}) - E_{MCR\text{-}Br}$$

$$\Delta E_2 = (E_U + E_{RF} + E_{Br}) - E_{MCR\text{-}Br}$$

$$\Delta\Delta E = \Delta E_2 - \Delta E_1 = E_U + E_{RF} - E_{MCR}$$

Using $\Delta\Delta E$, the relative tendency of midchain radical (MCR) to undergo β-scission into more stable fragments was investigated, where negative values indicate fragmentation products as more stable than their corresponding MCRs, whereas positive $\Delta\Delta E$ values indicate the opposite.

Total energies of substrates, intermediates, and final products along the activation-scission pathway were compared for their tendency to fragment. For computational efficiency and simplicity, the following assumptions were used:

1. Trends of fragmentation were explored broadly but reliably using trimeric substrates as opposed to extended penta-, hepta-, or *n*-meric (i.e., higher oligomeric or polymeric) structures.

2. Ester functionalities with oligo(ethylene oxide) substituent derived from $OEOA_{480}$, $OEOMA_{500}$, and OEOBA were simplified to the corresponding β-methoxyethyl ester models ($-CO_2CH_2CH_2OMe$), while comonomers and IB bearing $-CO_2Me$ ester moieties served as control model compounds.

3. For acrylate models, synthesized copolymers realistically would contain all possible stereochemical configurations neighboring their corresponding inibramer units, but their relative tendencies for fragmentation should all be similar (Figure S17, ESI).

Given these assumptions, the trends of fragmentation should be exhibited even within the model system by comparing acrylate- or methacrylate-based units flanking the OEOBA-derived inibramer. Indeed, similar symmetric "ABA" model substrates were analyzed by Yamago and coworkers for fragmentation selectivity in which a MCR moiety was flanked by two comonomer units, although with the branching point bearing a hydrogen or methyl and not ester, and not from the context of starting from any corresponding alkyl halide form.[77]

Fragmentation tendency inferred from total energies provided by calculations agreed with experimental fragmentation data based on the IB systems. Regardless of the inibramer-derived substituent within the acrylate model, all ΔE_2 values were considerably higher than their corresponding ΔE_1 values by ~24−35 kcal/mol, indicating unfavorable β-scission products (positive $\Delta\Delta E$ values) relative to their MCR analogs. Within the methacrylate model, positive $\Delta\Delta E$ values were found when the inibramer moiety was based on small substituents: methyl- and sodium 2-bromoacrylate (i.e., R = $-CO_2Me$ and $-CO_2-$, respectively, flanked with units bearing R_1 = CO_2Me). This indicates that copolymers of sodium 2-bromoacrylate with methyl acrylate or methacrylate would not appreciably fragment (Figure 7).

However, the inibramer model bearing an β-methoxyethyl variant (R = $-CO_2CH_2CH_2OMe$, mimicking OEOBA) with both methacrylate comonomers (R_1 = $-CO_2Me$ or $-CO_2CH_2CH_2OMe$) exhibited favorable fragmenting with ΔE_2 values lower than the corresponding ΔE_1 and thus the only negative $\Delta\Delta E$ values. Their negative $\Delta\Delta E$ values indicate favored β-scission products relative to their corresponding MCRs. This supports the observed tendency of $POEOMA_{500}$-*co*-POEOBA to undergo fragmentation upon halide activation during chain extension or branching conditions, where midchain halides could activate and fragment to generate lower molecular weight polymers. On the other hand, $POEOA_{480}$-*co*-POEOBA exhibited nonfragmenting MCRs and instead persisted to undergo addition to comonomer and create branching points, agreeing with the relatively high $\Delta\Delta E$ values found in the acrylate model.

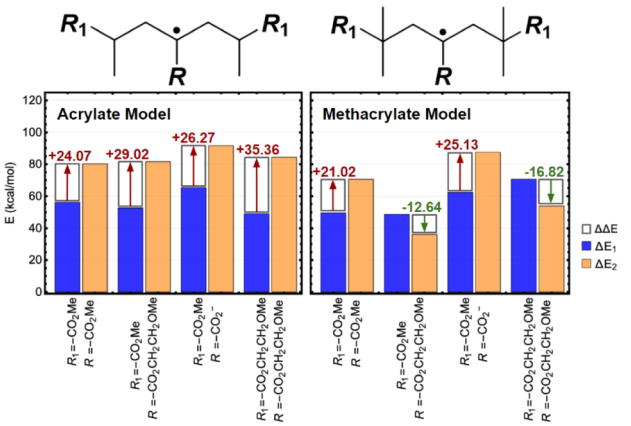

Figure 7. Corresponding ΔE_1, ΔE_2, and $\Delta\Delta E$ energies for substrates bearing different substituents (R derived from inibramer and R_1 from comonomer) in acrylate (left) and methacrylate (right) models. Values were obtained at the ωB97X-D4 def2-TZVP level of theory.

This limited study showed that methacrylate units flanking the OEOBA play a key role in favoring fragmentation products. Flanking acrylate units lead to unfavorable fragmentation products, regardless of the nature of the inibramer substituent. Furthermore, only methacrylate-based model compounds with inibramer units derived from the OEOBA (i.e., R = −CO2CH2CH2OMe) showed favorable β-scission products relative to their corresponding MCRs, as demonstrated by negative $\Delta\Delta E$ values. Future studies could include longer PEO substituents, more (co)monomer units appended to the substrate, and the addition of a solvent phase to the calculations. The use of model macromonomer, considerations regarding activation, the potential role of Cu, and the effect of stereochemistry are discussed in the electronic support information (ESI).

CONCLUSIONS

In conclusion, we have demonstrated successful synthesis and application of the novel oligo(ethylene oxide) methyl ether 2-bromoacrylate (OEOBA) IB toward the preparation of structurally controlled HB polyacrylates with the predetermined degree of branching, molecular weight, and architecture. Furthermore, the remarkable oxygen tolerance of green-light-induced dual EY/Cu-catalyzed ATRP, coupled with the fast kinetics and the retention of chain-end functionality, attests to the versatility of this technique in synthesis of topological block copolymers and HB-PPH. However, the incorporation of OEOBA in a polymethacrylate backbone resulted in backbone degradation under benign conditions. The computation studies revealed that flanking the inibramer with methacrylate units favored fragmentation products but only when employing an OEOBA-like IB. These findings emphasize the importance of IB and comonomer structures and highlight the potential for advancing CRBP methodologies, particularly in water. This research also contributes to expanding the toolkit of water-soluble IB and opens avenues for the tailored synthesis of intricate macromolecular structures with enhanced precision and efficiency.

https://doi.org/10.1021/acs.macromol.4c00408
Macromolecules 2024, 57, 5368−5379

■ ASSOCIATED CONTENT

Supporting Information

The Supporting Information is available free of charge at https://pubs.acs.org/doi/10.1021/acs.macromol.4c00408.

Experimental details including methods, instrumentation, and procedures, characterization results by SEC-MALS, details of computation methods and additional references (PDF)

■ AUTHOR INFORMATION

Corresponding Author

Krzysztof Matyjaszewski − *Department of Chemistry, Carnegie Mellon University, Pittsburgh, Pennsylvania 15213, United States;* orcid.org/0000-0003-1960-3402; Email: km3b@andrew.cmu.edu, matyjaszewski@cmu.edu

Authors

Kriti Kapil − *Department of Chemistry, Carnegie Mellon University, Pittsburgh, Pennsylvania 15213, United States*

Arman Moini Jazani − *Department of Chemistry, Carnegie Mellon University, Pittsburgh, Pennsylvania 15213, United States*

Julian Sobieski − *Department of Chemistry, Carnegie Mellon University, Pittsburgh, Pennsylvania 15213, United States*

Leticia P. Madureira − *Department of Chemistry, Carnegie Mellon University, Pittsburgh, Pennsylvania 15213, United States*

Grzegorz Szczepaniak − *Department of Chemistry, Carnegie Mellon University, Pittsburgh, Pennsylvania 15213, United States; Faculty of Chemistry, University of Warsaw, Warsaw 02-093, Poland;* orcid.org/0000-0002-0355-9542

Michael R. Martinez − *Department of Chemistry, Carnegie Mellon University, Pittsburgh, Pennsylvania 15213, United States; PPG Industries, Inc., Allison Park, Pennysylvania 15101, United States;* orcid.org/0000-0002-6211-763X

Adam Gorczyński − *Department of Chemistry, Carnegie Mellon University, Pittsburgh, Pennsylvania 15213, United States; Faculty of Chemistry, Adam Mickiewicz University, Poznań 61-614, Poland;* orcid.org/0000-0002-3930-8489

Hironobu Murata − *Department of Chemistry, Carnegie Mellon University, Pittsburgh, Pennsylvania 15213, United States*

Tomasz Kowalewski − *Department of Chemistry, Carnegie Mellon University, Pittsburgh, Pennsylvania 15213, United States;* orcid.org/0000-0002-3544-554X

Complete contact information is available at: https://pubs.acs.org/10.1021/acs.macromol.4c00408

Author Contributions

The manuscript was written through the contributions of all authors. All authors have given approval to the final version of the manuscript.

Funding

This work was supported by the NSF DMR 2202747 and Department of Threat Reduction Agency (DTRA) (grant HDTRA1-20-1-0014). A.M.J. acknowledges the Fonds de recherche du Québec (FRQNT) for financial support (File#301734).

Notes

The authors declare no competing financial interest.

■ REFERENCES

(1) Corrigan, N.; Jung, K.; Moad, G.; Hawker, C. J.; Matyjaszewski, K.; Boyer, C. Reversible-deactivation radical polymerization (Controlled/living radical polymerization): From discovery to materials design and applications. *Prog. Polym. Sci.* **2020**, *111*, 101311.

(2) Truong, N. P.; Jones, G. R.; Bradford, K. G. E.; Konkolewicz, D.; Anastasaki, A. A comparison of RAFT and ATRP methods for controlled radical polymerization. *Nat. Rev. Chem.* **2021**, *5*, 859−869.

(3) Perrier, S. 50th Anniversary Perspective: RAFT Polymerization—A User Guide. *Macromolecules* **2017**, *50*, 7433−7447.

(4) Shipp, D. A. Reversible-Deactivation Radical Polymerizations. *Polym. Rev.* **2011**, *51*, 99−103.

(5) Braunecker, W. A.; Matyjaszewski, K. Controlled/living radical polymerization: Features, developments, and perspectives. *Prog. Polym. Sci.* **2007**, *32*, 93−146.

(6) Wang, J. S.; Matyjaszewski, K. Controlled/"Living" Radical Polymerization. Halogen Atom Transfer Radical Polymerization Promoted by a Cu(I)/Cu(II) Redox Process. *Macromolecules* **1995**, *28*, 7901−7910.

(7) Patten, T. E.; Xia, J.; Abernathy, T.; Matyjaszewski, K. Polymers with very low polydispersities from atom transfer radical polymerization. *Science* **1996**, *272*, 866−868.

(8) Matyjaszewski, K.; Xia, J. H. Atom transfer radical polymerization. *Chem. Rev.* **2001**, *101*, 2921−2990.

(9) Matyjaszewski, K. Atom Transfer Radical Polymerization (ATRP): Current status and future perspectives. *Macromolecules* **2012**, *45*, 4015−4039.

(10) Gaynor, S. G.; Edelman, S.; Matyjaszewski, K. Synthesis of Branched and Hyperbranched Polystyrenes. *Macromolecules* **1996**, *29*, 1079−1081.

(11) Yan, D.; Müller, A. H. E.; Matyjaszewski, K. Molecular Parameters of Hyperbranched Polymers Made by Self-Condensing Vinyl Polymerization. 2. Degree of Branching. *Macromolecules* **1997**, *30*, 7024−7033.

(12) Matyjaszewski, K.; Miller, P. J.; Pyun, J.; Kickelbick, G.; Diamanti, S. Synthesis and Characterization of Star Polymers with Varying Arm Number, Length, and Composition from Organic and Hybrid Inorganic/Organic Multifunctional Initiators. *Macromolecules* **1999**, *32*, 6526−6535.

(13) Matyjaszewski, K. The synthesis of functional star copolymers as an illustration of the importance of controlling polymer structures in the design of new materials. *Polym. Int.* **2003**, *52*, 1559−1565.

(14) Sunder, A.; Heinemann, J.; Frey, H. Controlling the growth of polymer trees: Concepts and perspectives for hyperbranched polymers. *Chem. - Eur. J.* **2000**, *6*, 2499−2506.

(15) Imakaev, M. V.; Tchourine, K. M.; Nechaev, S. K.; Mirny, L. A. Effects of topological constraints on globular polymers. *Soft Mater.* **2015**, *11*, 665−671.

(16) Takata, T.; Aoki, D. Topology-transformable polymers: Linear-branched polymer structural transformation via the mechanical linking of polymer chains. *Polym. J.* **2018**, *50*, 127−147.

(17) Beers, K. L.; Gaynor, S. G.; Matyjaszewski, K.; Sheiko, S. S.; Möller, M. The synthesis of densely grafted copolymers by atom transfer radical polymerization. *Macromolecules* **1998**, *31*, 9413−9415.

(18) Gao, H. F.; Matyjaszewski, K. Synthesis of miktoarm star polymers via ATRP using the "in-out" method: Determination of initiation efficiency of star macroinitiators. *Macromolecules* **2006**, *39*, 7216−7223.

(19) Chremos, A.; Douglas, J. F. A comparative study of thermodynamic, conformational, and structural properties of bottlebrush with star and ring polymer melts. *J. Chem. Phys.* **2018**, *149*, 044904.

(20) Nian, S. F.; Huang, B. Q.; Freychet, G.; Zhernenkov, M.; Cai, L. H. Unexpected Folding of Bottlebrush Polymers in Melts. *Macromolecules* **2023**, *56*, 2551−2559.

(21) Matyjaszewski, K.; Gaynor, S. G.; Kulfan, A.; Podwika, M. Preparation of hyperbranched polyacrylates by atom transfer radical polymerization.1. Acrylic AB* monomers in"living" radical polymerizations. *Macromolecules* **1997**, *30*, 5192−5194.

(22) Matyjaszewski, K.; Gaynor, S. G. Preparation of hyperbranched polyacrylates by atom transfer radical polymerization.3. Effect of reaction conditions on the self-condensing vinyl polymerization of 2-((2-bromopropionyl)oxy)ethyl acrylate. *Macromolecules* **1997**, *30*, 7042−7049.
(23) Matyjaszewski, K.; Gaynor, S. G.; Muller, A. H. E. Preparation of hyperbranched polyacrylates by atom transfer radical polymerization.2. Kinetics and mechanism of chain growth for the self-condensing vinyl polymerization of 2-((2-bromopropionyl)oxy)ethyl acrylate. *Macromolecules* **1997**, *30*, 7034−7041.
(24) Cuthbert, J.; Beziau, A.; Gottlieb, E.; Fu, L. Y.; Yuan, R.; Balazs, A. C.; Kowalewski, T.; Matyjaszewski, K. Transformable Materials: Structurally Tailored and Engineered Macromolecular (STEM) Gels by Controlled Radical Polymerization. *Macromolecules* **2018**, *51*, 3808−3817.
(25) Cuthbert, J.; Balazs, A. C.; Kowalewski, T.; Matyjaszewski, K. STEM Gels by Controlled Radical Polymerization. *Trends Chem.* **2020**, *2*, 341−353.
(26) Poelma, J. E.; Ono, K.; Miyajima, D.; Aida, T.; Satoh, K.; Hawker, C. J. Cyclic Block Copolymers for Controlling Feature Sizes in Block Copolymer Lithography. *ACS Nano* **2012**, *6*, 10845−10854.
(27) Belgaonkar, M. S.; Kandasubramanian, B. Hyperbranched Polymer-based Nanocomposites: Synthesis, Progress, and Applications. *Eur. Polym. J.* **2021**, *147*, 110301.
(28) Kurniasih, I. N.; Keilitz, J.; Haag, R. Dendritic nanocarriers based on hyperbranched polymers. *Chem. Soc. Rev.* **2015**, *44*, 4145−4164.
(29) Chen, S.; Zhang, X. Z.; Cheng, S. X.; Zhuo, R. X.; Gu, Z. W. Functionalized Amphiphilic Hyperbranched Polymers for Targeted Drug Delivery. *Biomacromolecules* **2008**, *9*, 2578−2585.
(30) Wang, D.; Zhao, T.; Zhu, X.; Yan, D.; Wang, W. Bioapplications of hyperbranched polymers. *Chem. Soc. Rev.* **2015**, *44*, 4023−4071.
(31) Inoue, K. Functional dendrimers, hyperbranched and star polymers. *Prog. Polym. Sci.* **2000**, *25*, 453−571.
(32) Behera, G. C.; Ramakrishnan, S. Controlled variation of spacer segment in hyperbranched polymers: From densely branched to lightly branched systems. *Macromolecules* **2004**, *37*, 9814−9820.
(33) Jikei, M.; Kakimoto, M. Hyperbranched polymers: A promising new class of materials. *Prog. Polym. Sci.* **2001**, *26*, 1233−1285.
(34) Shao, G.; Li, A.; Liu, Y.; Yuan, B.; Zhang, W. Branched Polymers: Synthesis and Application. *Macromolecules* **2024**, *57*, 830−846.
(35) Voit, B. I.; Lederer, A. Hyperbranched and highly branched polymer architectures-synthetic strategies and major characterization aspects. *Chem. Rev.* **2009**, *109*, 5924−5973.
(36) Zheng, Y.; Li, S.; Weng, Z.; Gao, C. Hyperbranched polymers: Advances from synthesis to applications. *Chem. Soc. Rev.* **2015**, *44*, 4091−4130.
(37) Ohta, Y.; Fujii, S.; Yokoyama, A.; Furuyama, T.; Uchiyama, M.; Yokozawa, T. Synthesis of well-defined hyperbranched polyamides by condensation polymerization of AB2 monomer through changed substituent effects. *Angew. Chem., Int. Ed.* **2009**, *48*, 5942−5945.
(38) Flory, P. J. Molecular Size Distribution in Three Dimensional Polymers. VI. Branched Polymers Containing A-R-Bf-1 Type Units. *J. Am. Chem. Soc.* **1952**, *74*, 2718−2723.
(39) Hawker, C. J.; Lee, R.; Frechet, J. M. J. One-Step Synthesis of Hyperbranched Dendritic Polyesters. *J. Am. Chem. Soc.* **1991**, *113*, 4583−4588.
(40) Stiriba, S. E.; Kautz, H.; Frey, H. Hyperbranched molecular nanocapsules: Comparison of the hyperbranched architecture with the perfect linear analogue. *J. Am. Chem. Soc.* **2002**, *124*, 9698−9699.
(41) Chen, H.; Kong, J. Hyperbranched polymers from A_2 + B_3 strategy: Recent advances in description and control of fine topology. *Polym. Chem.* **2016**, *7*, 3643−3663.
(42) Alfurhood, J. A.; Bachler, P. R.; Sumerlin, B. S. Hyperbranched polymers: Via RAFT self-condensing vinyl polymerization. *Polym. Chem.* **2016**, *7*, 3361−3369.
(43) Wang, X.; Gao, H. Recent progress on hyperbranched polymers synthesized via radical-based self-condensing vinyl polymerization. *Polymers* **2017**, *9*, 188−188.
(44) Fréchet, J. M. J.; Henmi, M.; Gitsov, I.; Aoshima, S.; Leduc, M. R.; Grubbs, R. B. Self-condensing vinyl polymerization: An approach to dendritic materials. *Science* **1995**, *269*, 1080−1083.
(45) Sunder, A.; Hanselmann, R.; Frey, H.; Mülhaupt, R. Controlled synthesis of hyperbranched polyglycerols by ring-opening multibranching polymerization. *Macromolecules* **1999**, *32*, 4240−4246.
(46) Graff, R. W.; Wang, X.; Gao, H. Exploring Self-Condensing Vinyl Polymerization of Inimers in Microemulsion To Regulate the Structures of Hyperbranched Polymers. *Macromolecules* **2015**, *48*, 2118−2126.
(47) Min, K.; Gao, H. F. New Method To Access Hyperbranched Polymers with Uniform Structure via One-Pot Polymerization of Inimer in Microemulsion. *J. Am. Chem. Soc.* **2012**, *134*, 15680−15683.
(48) Ma, K. L.; Jin, X. Y.; Gan, W. P.; Fan, C. K.; Gao, H. F. Chain-growth click copolymerization for the synthesis of branched copolymers with tunable branching densities. *Polym. Chem.* **2022**, *13*, 891−897.
(49) Cao, X. S.; Shi, Y.; Wang, X. F.; Graff, R. W.; Gao, H. F. Design a Highly Reactive Trifunctional Core Molecule To Obtain Hyperbranched Polymers with over a Million Molecular Weight in One-Pot Click Polymerization. *Macromolecules* **2016**, *49*, 760−766.
(50) Shi, Y.; Graff, R. W.; Cao, X.; Wang, X.; Gao, H. Chain-Growth Click Polymerization of AB_2 Monomers for the Formation of Hyperbranched Polymers with Low Polydispersities in a One-Pot Process. *Angew. Chem.* **2015**, *127*, 7741−7745.
(51) Cao, M. X.; Zhong, M. J. Chain-growth branching radical polymerization: an inibramer strategy. *Polym. Int.* **2022**, *71*, 501−507.
(52) Lu, Y.; Nemoto, T.; Tosaka, M.; Yamago, S. Synthesis of structurally controlled hyperbranched polymers using a monomer having hierarchical reactivity. *Nat. Commun.* **2017**, *8*, 1863−1863.
(53) Li, F.; Cao, M.; Feng, Y.; Liang, R.; Fu, X.; Zhong, M. Site-Specifically Initiated Controlled/Living Branching Radical Polymerization: A Synthetic Route toward Hierarchically Branched Architectures. *J. Am. Chem. Soc.* **2019**, *141*, 794−799.
(54) Cao, M. X.; Liu, Y. T.; Zhang, X. W.; Li, F.; Zhong, M. J. Expanding the toolbox of controlled/living branching radical polymerization through simulation-informed reaction design. *Chem* **2022**, *8*, 1460−1475.
(55) Zhao, Y. C.; Ma, M. Y.; Lin, X. R.; Chen, M. Photoorganocatalyzed Divergent Reversible-Deactivation Radical Polymerization towards Linear and Branched Fluoropolymers. *Angew. Chem., Int. Ed.* **2020**, *59*, 21470−21474.
(56) Kapil, K.; Szczepaniak, G.; Martinez, M. R.; Murata, H.; Jazani, A. M.; Jeong, J.; Das, S. R.; Matyjaszewski, K. Visible-Light-Mediated Controlled Radical Branching Polymerization in Water. *Angew. Chem., Int. Ed.* **2023**, *62*, No. e202217658.
(57) Jiang, Y.; Kibune, M.; Tosaka, M.; Yamago, S. Practical Synthesis of Dendritic Hyperbranched Polyacrylates and Their Topological Block Polymers by Organotellurium-Mediated Emulsion Polymerization in Water. *Angew. Chem., Int. Ed.* **2023**, *62*, No. e202306916.
(58) Jones, G. R.; Anastasaki, A.; Whitfield, R.; Engelis, N.; Liarou, E.; Haddleton, D. M. Copper-Mediated Reversible Deactivation Radical Polymerization in Aqueous Media. *Angew. Chem., Int. Ed.* **2018**, *57*, 10468−10482.
(59) Oh, J. K.; Min, K.; Matyjaszewski, K. Preparation of poly(oligo(ethylene glycol) monomethyl ether methacrylate) by homogeneous aqueous AGET ATRP. *Macromolecules* **2006**, *39*, 3161−3167.
(60) Coca, S.; Jasieczek, C. B.; Beers, K. L.; Matyjaszewski, K. Polymerization of acrylates by atom transfer radical polymerization. Homopolymerization of 2-hydroxyethyl acrylate. *J. Polym. Sci., Part A: Polym. Chem.* **1998**, *36*, 1417−1424.
(61) Fantin, M.; Isse, A. A.; Matyjaszewski, K.; Gennaro, A. ATRP in Water: Kinetic Analysis of Active and Super-Active Catalysts for

https://doi.org/10.1021/acs.macromol.4c00408
Macromolecules 2024, 57, 5368−5379

Enhanced Polymerization Control. *Macromolecules* **2017**, *50*, 2696−2705.
(62) Braunecker, W. A.; Tsarevsky, N. V.; Gennaro, A.; Matyjaszewski, K. Thermodynamic Components of the Atom Transfer Radical Polymerization Equilibrium: Quantifying Solvent Effects. *Macromolecules* **2009**, *42*, 6348−6360.
(63) Junkers, T.; Barner-Kowollik, C. The Role of Mid-Chain Radicals in Acrylate Free Radical Polymerization: Branching and Scission. *J. Polym. Sci., Part A: Polym. Chem.* **2008**, *46*, 7585−7605.
(64) Fantin, M.; Isse, A. A.; Gennaro, A.; Matyjaszewski, K. Understanding the Fundamentals of Aqueous ATRP and Defining Conditions for Better Control. *Macromolecules* **2015**, *48*, 6862−6875.
(65) Szczepaniak, G.; Jeong, J.; Kapil, K.; Dadashi-Silab, S.; Yerneni, S. S.; Ratajczyk, P.; Lathwal, S.; Schild, D. J.; Das, S. R.; Matyjaszewski, K. Open-air green-light-driven ATRP enabled by dual photoredox/copper catalysis. *Chem. Sci.* **2022**, *13*, 11540−11550.
(66) Averick, S.; Simakova, A.; Park, S.; Konkolewicz, D.; Magenau, A. J. D.; Mehl, R. A.; Matyjaszewski, K. ATRP under biologically relevant conditions: Grafting from a protein. *ACS Macro Lett.* **2012**, *1*, 6−10.
(67) Olszewski, M.; Jeong, J.; Szczepaniak, G.; Li, S. P.; Enciso, A.; Murata, H.; Averick, S.; Kapil, K.; Das, S. R.; Matyjaszewski, K. Sulfoxide-Containing Polyacrylamides Prepared by PICAR ATRP for Biohybrid Materials. *ACS Macro Lett.* **2022**, *11*, 1091−1096.
(68) Fu, L. Y.; Jafari, H.; Giessl, M.; Yerneni, S. S.; Sun, M. K.; Wang, Z. Y.; Liu, T.; Kapil, K.; Cheng, B. C.; Yu, A.; et al. Grafting polymer brushes by ATRP from functionalized poly(ether ether ketone) microparticles. *Polym. Adv. Technol.* **2021**, *32*, 3948−3954.
(69) Kapil, K.; Jazani, A. M.; Szczepaniak, G.; Murata, H.; Olszewski, M.; Matyjaszewski, K. Fully Oxygen-Tolerant Visible-Light-Induced ATRP of Acrylates in Water: Toward Synthesis of Protein-Polymer Hybrids. *Macromolecules* **2023**, *56*, 2017−2026.
(70) Kapil, K.; Xu, S. R.; Lee, I. S.; Murata, H.; Kwon, S. J.; Dordick, J. S.; Matyjaszewski, K. Highly Sensitive Detection of Bacteria by Binder-Coupled Multifunctional Polymeric Dyes. *Polymers* **2023**, *15*, 2723.
(71) Tosaka, M.; Takeuchi, H.; Kibune, M.; Tong, T. X.; Zhu, N. Y.; Yamago, S. Stochastic Simulation of Controlled Radical Polymerization Forming Dendritic Hyperbranched Polymers. *Angew. Chem., Int. Ed.* **2023**, *62*, No. e202305127.
(72) Voit, B. New developments in hyperbranched polymers. *J. Polym. Sci., Part A: Polym. Chem.* **2000**, *38*, 2505−2525.
(73) Kapil, K.; Murata, H.; Szczepaniak, G.; Russell, A. J.; Matyjaszewski, K. Tailored Branched Polymer−Protein Bioconjugates for Tunable Sieving Performance. *ACS Macro Lett.* **2024**, *13*, 461−467.
(74) Li, S. P.; Chung, H. S.; Simakova, A.; Wang, Z. Y.; Park, S.; Fu, L. Y.; Cohen-Karni, D.; Averick, S.; Matyjaszewski, K. Biocompatible Polymeric Analogues of DMSO Prepared by Atom Transfer Radical Polymerization. *Biomacromolecules* **2017**, *18*, 475−482.
(75) Szczepaniak, G.; Piatkowski, J.; Nogas, W.; Lorandi, F.; Yerneni, S. S.; Fantin, M.; Ruszczynska, A.; Enciso, A. E.; Bulska, E.; Grela, K.; et al. An isocyanide ligand for the rapid quenching and efficient removal of copper residues after Cu/TEMPO-catalyzed aerobic alcohol oxidation and atom transfer radical polymerization. *Chem. Sci.* **2020**, *11*, 4251−4262.
(76) Beckingham, B. S.; Sanoja, G. E.; Lynd, N. A. Simple and Accurate Determination of Reactivity Ratios Using a Nonterminal Model of Chain Copolymerization. *Macromolecules* **2015**, *48*, 6922−6930.
(77) Lu, Y.; Yamago, S. Synthesis of Structurally Controlled, Highly Branched Polymethacrylates by Radical Polymerization through the Design of a Monomer Having Hierarchical Reactivity. *Macromolecules* **2020**, *53*, 3209−3216.
(78) Ma, Y.; Zhao, Y. N.; Yang, X. M.; Li, J. F.; Wang, X. Y.; Tang, Y. SaBOX/Copper-Catalyzed Synthesis, Degradation, and Upcycling of a PMMA-Based Copolymer. *Macromolecules* **2023**, *56*, 7032−7042.
(79) Ballard, N.; Salsamendi, M.; Santos, J. I.; Ruipérez, F.; Leiza, J. R.; Asua, J. M. Experimental Evidence Shedding Light on the Origin of the Reduction of Branching of Acrylates in ATRP. *Macromolecules* **2014**, *47*, 964−972.
(80) Kimura, T.; Kuroda, K.; Kubota, H.; Ouchi, M. Metal-Catalyzed Switching Degradation of Vinyl Polymers via Introduction of an "In-Chain" Carbon-Halogen Bond as the Trigger. *ACS Macro Lett.* **2021**, *10*, 1535−1539.
(81) Cakir, Y. B.; Kiliclar, H. C.; Yagci, Y. Metal free, white LED induced, room temperature degradation of methyl methacrylate-Methyl haloacrylate copolymers. *React. Funct. Polym.* **2023**, *191*, 105656.
(82) Arslan, Z.; Kiliclar, H. C.; Yagci, Y. Visible Light Induced Degradation of of Poly(methyl methacrylate-co-methyl α-chloro acrylate) Copolymer at Ambient Temperature. *Macromol. Rapid Commun.* **2023**, *44*, 2300066.
(83) Jazani, A. M.; Arezi, N.; Maruya-Li, K.; Jung, S.; Oh, J. K. Facile Strategies to Synthesize Dual Location Dual Acidic pH/Reduction-Responsive Degradable Block Copolymers Bearing Acetal/Disulfide Block Junctions and Disulfide Pendants. *ACS Omega* **2018**, *3*, 8980−8991.
(84) Bian, C.; Zhou, Y. N.; Guo, J. K.; Luo, Z. H. Aqueous Metal-Free Atom Transfer Radical Polymerization: Experiments and Model-Based Approach for Mechanistic Understanding. *Macromolecules* **2018**, *51*, 2367−2376.
(85) Fantin, M.; Lorandi, F.; Ribelli, T. G.; Szczepaniak, G.; Enciso, A. E.; Fliedel, C.; Thevenin, L.; Isse, A. A.; Poli, R.; Matyjaszewski, K. Impact of Organometallic Intermediates on Copper-Catalyzed Atom Transfer Radical Polymerization. *Macromolecules* **2019**, *52*, 4079−4090.

https://doi.org/10.1021/acs.macromol.4c00408
Macromolecules 2024, 57, 5368−5379